ECRH scenarios with transition from X2 to O2 mode in W7-X Stellarator

N.B. Marushchenko, C. Beidler, V. Erckmann, J. Geiger, H. Laqua, H. Maassberg, Y. Turkin

Max Planck Institute for Plasma Physics, Wendelsteinstr. 1, D-17491 Greifswald, Germany

Introduction

In the W7-X stellarator [1], the system for electron cyclotron resonance heating (ECRH) is designed for continuous operation [2, 3] with a total injected power up to 10 MW at 140 GHz (the resonance magnetic field is $B_0 = 2.5$ T). The heating scheme for low and moderate densities, $n_e < 1.2 \times 10^{20}$ m^{-3}, uses the 2nd harmonic extraordinary mode (X2 scenario), and for higher densities, up to $n_e < 2.0 \times 10^{20}$ m^{-3}, the multi-pass scheme at the 2nd harmonic ordinary mode (O2 scenario) has to be applied. While the operation with the X2-mode is studied well, the scenarios with O2-mode require a big attention. A peculiarity of the O2 scheme is that it requires the start-up and preheating with the X2 scheme followed by changing the polarization of the RF wave-beam and ramping-up the density.

Contrary to the X2-mode, where the location of deposition is defined mainly by the resonance magnetic field, the O2 scenario is very sensitive also for the density and temperature profiles. Apart from this, the finite-β effects shift the magnetic equilibrium and also make a changing of location of the deposition profile. As consequence, conditions for the central heating for X2 and O2 are different [4]. Magnetic field necessary for the central deposition of the O2-mode corresponds to the shifted in low-field-side (LFS) direction X2 deposition. An other important problem for transition is also the density control. As an option, the pellet injection can be used.

The "standard" magnetic configuration optimized for confinement is suitable well for operation with the X2-mode, where the bootstrap current can be compensated by ECCD (completely for low densities and marginally for moderate ones), for the O2-mode, where ECCD is strongly reduced, this configuration is not favorable. Instead, the "high-mirror" magnetic configuration can be chosen from the configuration space of W7-X [5] as most relevant for high-density operation with the O2-mode since the bootstrap current for this kind of configuration is only small. As an example for modeling X2→O2 transition, the "high-mirror" configuration with 11% of B/B_{00} modulation is chosen.

Simulations were performed by the 1D-transport code `NTSS` [6] using comprehensive neoclassical and simple turbulent transport models, which is coupled with the ray-tracing code `TRAVIS` [7]. In order to account the finite-β effects and possible change of the rotational transform, ι, profile, the magnetic equilibrium is iteratively recalculated by the `VMEC` code [8] as well as the transport coefficients recalculated by the `DKES` code [9].

Simulation of X2→O2 transition

For modeling, the X2 scenario with 5 MW of ECR heating with the LFS-shifted deposition profile is considered. Since the complete absorption of the O2-mode can be happen only after several passes of the RF beam through the plasma, five RF beams 1 MW each are directed to the mirrors in the inner wall. The magnitude of magnetic field is adjusted for central heating by the O2-mode, and the resulting deposition of the X2-mode appears LFS-shifted: for steady-state with $\langle\beta\rangle \simeq 2\%$ the X2-deposition is located near $\rho \simeq 0.4$ (in the vacuum magnetic configuration the resonance $B = 2.5$ T appears near $\rho = 0.75$; here, $\rho = r_{\rm eff}/a$, respectively).

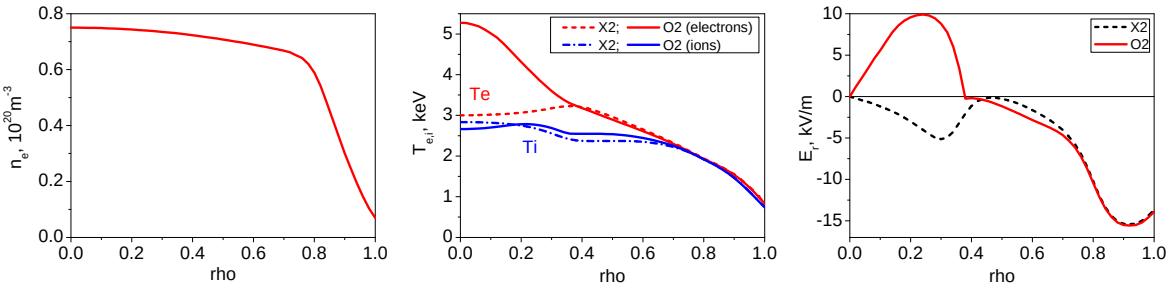

Figure 1: *Plasma profiles for the X2 and O2 steady-states. Dashed lines indicate the profiles for the X2-mode and the solid lines - for the O2-mode. Left: density n_e. Middle: temperatures T_i (blue) and T_e (red). Right: radial electric field, E_r.*

For simulations, the density $n_e(0) = 0.75 \times 10^{20}$ m^{-3} with the fixed profile (see see Fig. 1, left) and $Z_{\rm eff} = 1.5$ with the impurity C^{+6} are taken. For obtaining the initial plasma profiles for the transition, several iterations were performed: after establishing the temperature and ι-profiles, a new magnetic equilibrium and new transport coefficients were calculated, followed by a run of the transport code.

The plasma profiles for the X2-mode, n_e, $T_{e,i}$ and E_r, are shown in Fig. 1 by dashed lines. One can find that due to the LFS-shifted deposition (Fig. 2, left), $T_{e,i}$-profiles for X2 scenario are practically flat in the central domain and the negative radial electric field is defined by the "ion-root" (i-root) solution. Since both the bootstrap current and ECCD are sufficiently small (the current profiles are shown Fig. 2, middle), $I_{bc}^{X2} = 5.0$ kA and $I_{eccd}^{X2} = -1.65$ kA, the residual current satisfies well the requirement for successful operation of the divertor, $|I_{bc} + I_{eccd}| <$ 10 kA [3] and the edge value of ι is practically unaffected (see Fig. 2, right).

For "converged" the steady-state X2 scenario, the polarization of the RF beams is changed from extraordinary to ordinary wave-mode. Since the plasma is optically gray for the O2-mode, i.e. $\tau_{O2} \sim 1$ for the single pass, the multi-pass scenario is necessary (for the first reflection, the inner wall is equipped with mirrors). For the considered case, three passes are sufficient for practically complete absorption. With the O2-mode, the same iteration loop was performed: the

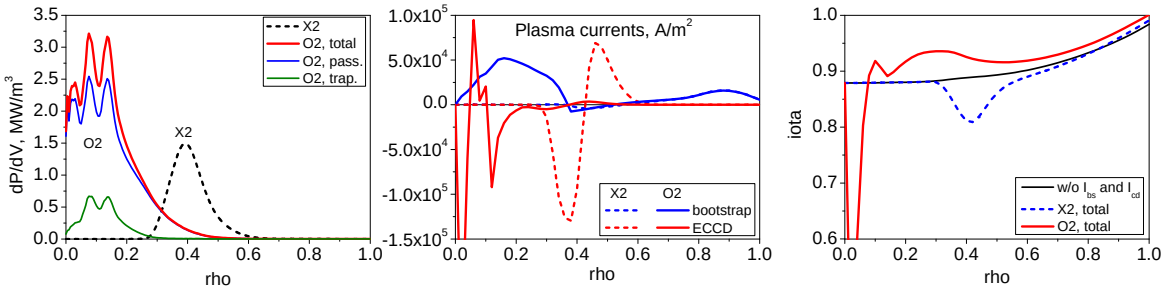

Figure 2: *Left: $dP_{\rm abs}/dV$ for both X2 (black) and O2-modes (red) with contributions from passing (blue) and trapped (green) electrons). Middle: bootstrap current profiles (blue) with $I_{bc}^{X2} = 5.0$ kA and $I_{bc}^{O2} = 8.65$ kA, and ECCD (red) with $I_{eccd}^{X2} = -1.65$ kA and $I_{eccd}^{O2} = -0.89$ kA. Right: ι-profiles with (blue and red) and w/o plasma currents (black) accounted.*

equilibrium was recalculated by VMEC with the new β-profile and then the transport coefficients were obtained by DKES. The new run of the transport code NTSS with the new data give the new steady state. The obtained plasma profiles are shown in Fig. 1 by solid lines.

As expected, the deposition profile for the O2-mode is much broader than for the X2-mode and located in the central domain; see Fig. 2, left. The main changing which appears after transition from off-axis X2 to the O2 scenario with the central heating is an establishing in the heated domain of the "electron-root" (e-root) with the positive electric field and improved confinement (see Fig. 1, right, red line). As result, T_e-profile becomes peaked with significant increasing from $T_e(0) \simeq 3.0$ keV for X2 to $T_e(0) \simeq 5.3$ keV for O2-mode (Fig. 1, middle) with practically unchanged T_i-profile. The bootstrap current is also somewhat increased, $I_{bc}^{O2} = 8.65$ kA, but ECCD despite of increasing of T_e, is further reduced, $I_{eccd}^{O2} = -0.89$ kA. However, the residual current is still within the requirements and the changing of the edge value of ι is acceptable (see Fig. 2, middle and right).

Significant reduction of ECCD for O2 is happening due to the following reasons. Contrary to the X2-mode, contribution of the trapped electrons in multi-pass absorption of the O2-mode is non-negligible, and about 12% of power is deposited in the trapped electrons. Additionally, also the Ohkawa counter-current appears that also leads to significant reduction of ECCD.

For transition to O2 operation, the equilibrium was recalculated only with the β-profile accounted and disturbance of the ι-profile, which is strongest within the narrow magnetic tube near the axis, was ignored for few reasons. First of all, due to discretization of the RF beams by the rays, the deposition and current drive profiles near the axis cannot be sufficiently accurate and the artefacts like a "spikes" near axis in the j_{eccd}-profile can appear. Apart from this, it is necessary to stress that the obtained steady state with the O2-mode for the density $n_e(0) = 0.75 \times 10^{20}$ m^{-3} is not considered as scenario for long pulses. This steady-state is in

fact only the intermediate point before the densities ramped up to values above the X2-mode cut-off, 1.2×10^{20} m^{-3}.

While the deposition and plasma profiles after changing from X2 to O2 are establishing within the energy confinement time, $\tau_E \simeq 0.35$ sec, the characteristic time for establishing the plasma current profile (bootstrap current and ECCD and the inductive screening current) is defined by the diffusive skin-time, $\tau_D \simeq 4$ sec. Finally, the relaxation of the loop-voltage happens in L/R time, which is about of 20 sec. The magnetic equilibrium reacts for changes also with these characteristic times: the fastest reaction with τ_E time is coming from the finite-β effects, i.e. the diamagnetic effect and Shafranov shift are established together with the temperature profiles, but the ι-profile is establishing much slowly, with the skin time. Since the density ramping up (or the pellet injection) must be started immediately after changing the polarization, in simulation of transition only the fastest processes need to be accounted, i.e. the finite-β effects. However, the dynamic of this process requires a more complicated modeling.

Summary

Summarizing the results for simulation of transition from the X2 to O2 operation with the "high-mirror" magnetic configuration, one can conclude that the intermediate steady state with the O2-mode, calculated by the iterative transport modeling, can be established well for the moderate density suitable for both X2 and O2-modes. In order to guarantee on-axis heating for the O2-mode, the X2 scenario with strongly LFS-shifted deposition profile needs to be applied. For both X2 and O2 wave-modes, the buutstrap current as well as the current drive are small and the residual current satisfy the conditions for divertor operation. Since for O2 operation the density ramping up must be done after changing the polarization of the RF beams as fast as possible, only the finite-β effects need to be accounted in iterative calculatiions of the magnetic equilibrium during the X2$\rightarrow$O2 transition.

References

[1] G. Grieger *et al.*, Phys. Fluids B **4**, 2081 (1992)

[2] V. Erckmann *et al.*, Plasma Sci. Technol. **52**, 291 (2007)

[3] J. Geiger *et al.*, Plasma Phys. Control. Fusion **55**, 014006 (2013)

[4] N.B. Marushchenko *et al.*, EPJ Web of Conferences **32**, 01004 (2012)

[5] J. Geiger *et al.*, Plenary talk in this conf., 41st EPS, I1.001 (2014)

[6] Y. Turkin *et al.*, Phys. Plasmas **18**, 022505 (2011)

[7] N.B. Marushchenko, Y. Turkin, and H. Maassberg, Comp. Phys. Comm. **185**, 165 (2014)

[8] S.P. Hirshman and J.C. Whitson, Phys. Fluids **26**, 3553 (1983)

[9] S.P. Hirshman *et al.*, Phys. Fluids **29**, 2951 (1986)